Inorganic Chemistry

Communication

pubs.acs.org/IC

Electronic Structure of Open-Shell Tetrahedral $\{Fe(NO)_2\}^9$ Dinitrosyliron Complexes

Kuan-Yu Liu[†] and Jen-Shiang K. Yu*[,†,‡]

[†]Department of Biological Science and Technology and [‡]Institute of Bioinformatics and Systems Biology, National Chiao Tung University, Hsinchu 30013, Taiwan

Supporting Information

ABSTRACT: High-level ab initio excited-state theory is employed to investigate the electronic structure of doublet $\{Fe(NO)_2\}^9$ species in the ground state and compared with the results obtained by density functional theory. Both of the approaches consistently suggest that the linear NO ligands in dinitrosyliron complexes (DNICs) feature a radical character. Theoretical calculations also predict that the cyanide-supported DNIC anion of $[(NC)_2Fe(NO)_2]^-$ features C_{2v} symmetry with a Fe−C−N bonding motif, and multireference theories suggest a minimal active space of CAS(9,9) to describe these $\{Fe(NO)_2\}^9$ compounds, while larger CAS(13,13) calculations do not tend to significantly improve the geometries. Experimental vibration modes of NO ligands are also accurately assigned due to second-order n-electron valence state perturbation theory.

Dinitrosyliron complexes (DNICs) were initially characterized in animal and yeast cells with thiolato ligands a half-century ago.[1−4] The biological significance of DNICs and derivatives received continual attention after the discovery of an alternative nitric oxide (NO) source in biological systems as L-arginine by Ignarro and Vanin.[5,6] In DNICs, iron atoms are four-coordinate and adopt a tetrahedral geometry. Four possible electronic structures of DNICs have been proposed to account for the oxidation state of $[Fe(NO)_2]^+$, in terms of $Fe^I(NO^\bullet)_2$,[7−9] $Fe^{I-}(NO^+)_2$,[10,11] resonance hybrids of $Fe^I(NO)_2$ and $Fe^{III}(NO^-)_2$,[12,13] and resonance hybrids of $Fe^{III}(NO^-)_2$ and $Fe^{II}(NO)_2^-$.[14,15] In recognition of the covalent and extensive delocalization in interactions such as Fe−N−O, Enemark and Feltham suggested a widely used notation, the E−F notation,[16] which treats the metal nitrosyl as a single unit in terms of the electron count. $[Fe(NO)_2]^+$, for example, is denoted by $\{Fe(NO)_2\}^9$, where 9 is the total number of electrons associated with the d electrons of iron and the π^* electrons of NO.

$\{Fe(NO)_2\}^9$ DNICs featuring several ligands along the spectrochemical series have been reported for individual features and may function for specific biological purposes. Bryar and Eaton studied the structure and coordination of the complex $[I_2Fe(NO)_2]^-$ (**1**)[10] as one of the DNICs containing simple anions. Later, in a chemically designed system, Tsai et al. analyzed DNICs with S/N/O ligation including azide-coordinated $[(N_3)_2Fe(NO)_2]^-$ (**2**).[17] Inspired by the phenomenon that the nitroxyl anion (NO^-) regulates smooth muscle of normal and cardiac hearts in vivo, an interesting homoleptic compound, $[(NO)_2Fe(NO)_2]^-$ (**3**), which is supported by four nonequivalent NO ligands, has been synthesized by Liaw and co-workers.[18] High-level ab initio calculations have also been carried out to study the electronic structure of **3**. Hsieh et al.[19] later synthesized the thiocyanate-ligated DNIC $[(SCN)_2Fe(NO)_2]^-$ (**4**) and investigated its electronic structure in the motif of $\{Fe(NO)_2\}^9$ associated with possible linkage isomerism of these SCN^- ligands.

Cyanide (CN^-), on the other hand, is a functional industrial chemical, but its excellent coordination ability leads to fatal toxification in live organs. The cyano-bound DNIC $[(NC)_2Fe(NO)_2]^-$ (**5**) has been proposed as one of the intermediate molecules in the decomposition mechanisms of the one-electron reduction product of nitroprusside ion, $[Fe(CN)_5NO]^{2-}$.[20] The structure of **5**, however, has not yet been experimentally realized because of difficulty isolating such transient species, yet spectral evidence supports its existence. We therefore became interested in the geometries and electronic structures of these open-shell anionic $\{Fe(NO)_2\}^9$ DNICs by theoretical methods. Accordingly, density functional theory (DFT) and wave function approaches were employed to assess their accuracy and capability in the prediction of the structural motif for novel DNICs.

DFT calculations employing generalized gradient approximation (GGA) using BP86 (DFT with Becke88 exchange and Perdew86 correlation functionals) functionals[21] and meta-GGA functionals of TPSS (exchange functional of Tao, Perdew, Staroverov, and Scuseria) and TPSSh (its hybrid version),[22] as well as the ab initio symmetry-adapted cluster/configuration interaction (SAC−CI)[23] approach, are used to perform geometry optimizations for **1**−**5**. (The Supporting Information, SI, provides computational details.) The optimized geometries of **1**, **2**, and **4** are shown in Figure 1 (and are detailed in Tables S1−S5 in the SI).

Single-reference methods are able to give consistent and accurate structural parameters for **1**, **2**, and **4**. X-ray crystal structures indicate that **1** and **4** adopt nearly C_{2v} symmetry, while **2** is C_2-symmetric. It is noticed that DFT calculations converge the geometry of **2** into virtually C_{2v} symmetry, although the symmetry constraint is not imposed during optimization (Tables S1 and S4 in the SI). For **1**, **2**, and **4**, the benchmarked DFT methods adequately predict the geometries, while pure GGA functionals possess the least spin contamination. An excited-state approach at the SAC−CI level also successfully reproduces

Received: January 21, 2014
Published: October 3, 2014

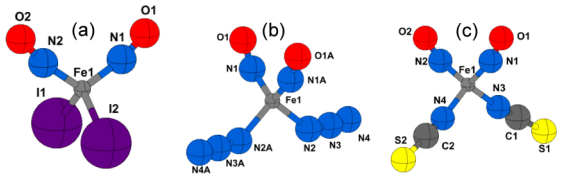

Averaged	BP86	SAC-CI	Exptl.	BP86	SAC-CI	Exptl.	BP86	SAC-CI	Exptl.
Fe-N	1.646	1.643	1.681	1.656	1.660	1.693	1.661	1.703	1.700
N-O	1.190	1.145	1.145	1.195	1.164	1.172	1.190	1.164	1.170
Fe-N-O	168.4	167.6	165.9	162.9	161.0	160.7	162.0	162.4	161.8

Figure 1. Selected bond lengths (Å) and bond angles (deg) for optimized geometries of $\{Fe(NO)_2\}^9$ DNICs containing (a) I^- (**1**), (b) N_3^- (**2**), and (c) SCN^- (**4**). See also the SI for details.

experimental structures for all of **1**−**4**, and these DFTs are able to optimize the geometries except for homoleptic **3**.

Multireference calculations at the levels of complete active-space self-consistent field (CASSCF)[24] as well as its second-order perturbative correction using n-electron valence state perturbation theory (NEVPT2)[25], are additionally employed to investigate these DNICs, and all of the experimental structures are satisfactorily reproduced. At the NEVPT2 level, it incorporates dynamic correlation and thus improves the Fe−N bond lengths by shrinking the interatomic distances, while the CASSCF theory tends to overestimate them.[26] The wave functions of these DNICs exhibit a dominant anionic configuration whose CI coefficient is about 0.7. For the homoleptic **3**, its major CI coefficient at NEVPT2(9,9) is 0.68, alone with another nine minor configurations greater than 1% as well as 34 other very diffused expansions (Figures 2 and S3 in the

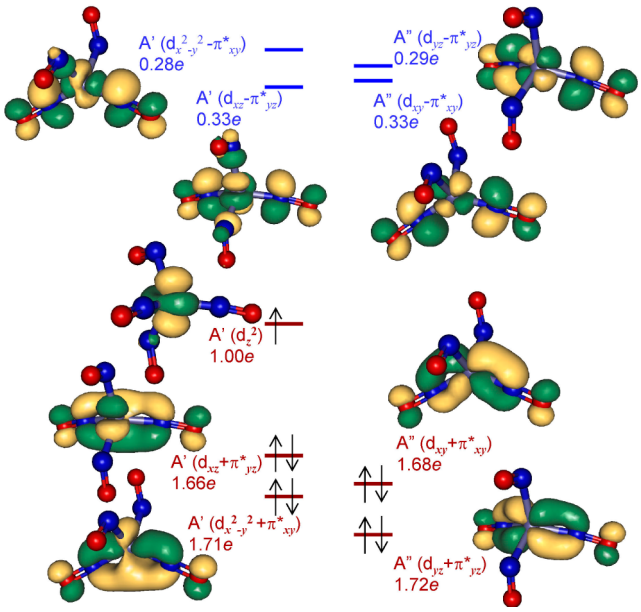

Figure 2. Nature orbital diagram of **3** at NEVPT2(9,9).

SI) of which CI coefficients are larger than 0.05. Within the active space, the sum of the occupation numbers of each bonding−antibonding orbital pair of the same character is very close to two electrons, consistent with the findings in the literature.[27] In addition, charge analyses[27] based on Boys orbital localization in the CAS(9,9) wave function assign iron a numerical charge of 2.61+, which is principally composed of Fe^{II} (39%) and Fe^{III} (52%) (Figure S6 in the SI).

It is also demonstrated in Table S3 in the SI that larger active spaces of CAS(13,11) and CAS(13,13) do not yield significant superior geometries compared to those obtained with CAS(9,9); in addition, their converged spin density plots may also indicate that under symmetry constraint the active space of CAS(9,9) is sufficient to describe the $\{Fe(NO)_2\}^9$ system.[28] Orbital localization of **3** using the larger CAS(13,13) space gives iron a slightly less positive numerical charge of 2.23+ (Figures S7 and S8 in the SI), with increased Fe^{II} (51%) and decreased Fe^{III} (33%) ratios compared to those of CAS(9,9). Experimental vibration frequencies of the two NO ligands of the DNICs are also excellently identified at the NEVPT2 level by harmonic frequency calculations, and meanwhile CASSCF theory obviously overestimates the numerics (Table S6 in the SI).

Geometry optimizations for **3** were not successful using DFT possibly because of the fact that density functionals failed to generate adequate spin density in this homoleptic system, while spin density plots of **1**, **2**, **4**, and **5** produced by both DFT and multireference theories are consistent (Figure S11 in the SI); similar conclusions have also been reported by Reiher and co-workers.[28,29] The geometrical parameters of **5** predicted by DFT, ab initio SAC−CI, and multireference calculations agree mutually and favor C_{2v} symmetry (Tables 1 and S5 in the SI), and the CASSCF orbital diagrams are essentially tantamount regardless of the symmetry. All of the quantum mechanical approaches unanimously suggest the Fe−C−N bonding units and foretell the average bond length between the iron and nitrogen atoms (of the NO ligand) at around 1.65−1.75 Å with an almost-linear Fe−N−O bond angle of 165° on average. The orbital diagram of C_{2v}-symmetric **5** (Figure S5 in the SI) reveals that its electronic configuration is akin to the other four DNICs, with the singly occupied molecular orbital being an unpaired electron localized at the d_{z^2} orbital of iron, while the two other pairs of mutually perpendicular (d,π^*) hybridized orbitals as well as their antibonding rivals are all composed of iron and the two NO ligands; their energetic orders might vary because of the different anions in each compound. All of the orbital diagrams illustrate the foresight of Enemark and Feltham to enclose the metal nitrosyl as a single entity in the coordination.

The charge distributions of **3**−**5** are demonstrated in Figure 3 by the electrostatic potential (ESP) maps based on the optimized geometries (those of **1** and **2** shown in Figure S9 in the SI). Negative charge distributions are concentrated on the iodo (**1**), azido (**2**), bent NO (**3**), thiocyano (**4**), and cyano (**5**) ligands, and all of the linear nitrosyls among the five DNICs behave more similar to neutral radicals.

The spectroscopic features of **5** reported in the literature are also recreated by theoretical calculations. The experimental frequencies[20] of **5** at 1810 and 1737 cm^{-1} are assigned as NO stretching bands due to the excellently agreeable theoretical values of 1857 cm^{-1} (symmetric) and 1785 cm^{-1} (asymmetric), respectively, at the NEVPT2(9,9) level, while CASSCF(9,9) overestimates them at 2103 and 1987 cm^{-1}.

In conclusion, DFT calculations seemingly fail to account for the accurate spin density for homoleptic **3** and lead to incorrect geometry optimization, while the high-level ab initio excited-state approach of SAC−CI as well as multireference methods can be applied for such conditions and well reproduce experimental geometries for all of the five tested open-shell DNIC anions. The molecular structure of transient intermediate **5** is consistently predicted by all of the DFT, SAC−CI, CASSCF, and NEVPT2 methods with an Fe−C−N bond angle of ∼165°. In addition, the recommended minimal active space of CAS(9,9) is sufficiently

dx.doi.org/10.1021/ic501116t | Inorg. Chem. 2014, 53, 10785−10787

Table 1. Optimized Geometrical Parameters of 5 at the DFT and ab Initio Levels

	BP86	SAC−CI		CASSCF(9,9)	NEVPT2(9,9)
	C_1	C_2	C_{2v}	C_1	C_{2v}
Fe−N(NO) (Å)	1.649	1.648	1.687	1.751	1.747
N−O (Å)	1.189	1.164	1.168	1.145	1.189
Fe−C (Å)	1.947	1.906	2.011	2.125	2.064
C−N (Å)	1.186	1.234	1.170	1.148	1.197
∠Fe−N−O (deg)	172.1	160.8	169.3	162.5	162.7
∠Fe−C−N (deg)	179.2	141.2	178.9	179.0	180.0

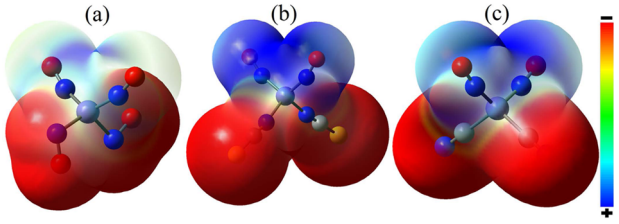

Figure 3. Charge distributions of compounds **3**−**5** demonstrated by ESP maps.

appropriate to describe the structures of these $\{Fe(NO)_2\}^9$ species using multireference approaches under symmetry constraint. These assessments may be beneficial to investigating novel DNICs or other open-shell anionic coordination systems.

■ ASSOCIATED CONTENT

Supporting Information

Details of theoretical calculations and results. This material is available free of charge via the Internet at http://pubs.acs.org.

■ AUTHOR INFORMATION

Corresponding Author

*E-mail: jsyu@mail.nctu.edu.tw.

Author Contributions

All authors have given approval to the final version of the manuscript.

Notes

The authors declare no competing financial interest.

■ ACKNOWLEDGMENTS

We are grateful to the Ministry of Science and Technology, Taiwan, for financial support under Grants NSC 100-2627-B-009-001, MOST 102-2113-M-009-013, and MOST 103-2113-M-009-014-MY3 and the "Center for Bioinformatics Research of Aiming for the Top University Program" of NCTU and MoE, Taiwan. We thank Professor Hiroshi Nakatsuji and colleagues at the Quantum Chemistry Research Institute, Japan, as well as Professor Henryk Witek in the Department of Applied Chemistry, National Chiao Tung University, Taiwan, respectively, for useful discussions on the SAC−CI and multireference computations.

■ REFERENCES

(1) Mallard, J. R.; Kent, M. *Nature* **1964**, *204*, 1192.
(2) Vanin, A. F.; Blumenfeld, L. A.; Chetverikov, A. G. *Biofizika* **1967**, *12*, 829−841.
(3) Vanin, A. F.; Nalbandyan, R. M. *Biofizika* **1965**, *10*, 167−168.
(4) Vithaythil, A. J.; Ternberg, J. L.; Commoner, B. *Nature* **1965**, *207*, 1246−1249.
(5) Ignarro, L. J. *Nitric Oxide Biology and Pharmacology*; Academic Press: San Diego, CA, 2000.
(6) Vanin, A. F. *Nitric Oxide-Biol. Ch.* **2009**, *21*, 1−13.
(7) Dai, R. J.; Ke, S. C. *J. Phys. Chem. B* **2007**, *111*, 2335−2346.
(8) Foster, M. W.; Cowan, J. A. *J. Am. Chem. Soc.* **1999**, *121*, 4093−4100.
(9) Tsai, M. L.; Chen, C. C.; Hsu, I. J.; Ke, S. C.; Hsieh, C. H.; Chiang, K. A.; Lee, G. H.; Wang, Y.; Chen, J. M.; Lee, J. F.; Liaw, W. F. *Inorg. Chem.* **2004**, *43*, 5159−5167.
(10) Bryar, T. R.; Eaton, D. R. *Can. J. Chem.* **1992**, *70*, 1917−1926.
(11) Butler, A. R.; Megson, I. L. *Chem. Rev.* **2002**, *102*, 1155−1165.
(12) Hopmann, K. H.; Ghosh, A.; Noodleman, L. *Inorg. Chem.* **2009**, *48*, 9155−9165.
(13) Tsai, M.-C.; Tsai, F.-T.; Lu, T.-T.; Tsai, M.-L.; Wei, Y.-C.; Hsu, I. J.; Lee, J.-F.; Liaw, W.-F. *Inorg. Chem.* **2009**, *48*, 9579−9591.
(14) Tsou, C.-C.; Tsai, F.-T.; Chen, H.-Y.; Hsu, I. J.; Liaw, W.-F. *Inorg. Chem.* **2013**, *52*, 1631−1639.
(15) Ye, S.; Neese, F. *J. Am. Chem. Soc.* **2010**, *132*, 3646−3647.
(16) Enemark, J. H.; Feltham, R. D. *Coord. Chem. Rev.* **1974**, *13*, 339−406.
(17) Tsai, M.-L.; Hsieh, C.-H.; Liaw, W.-F. *Inorg. Chem.* **2007**, *46*, 5110−5117.
(18) Lin, Z.-S.; Chiou, T.-W.; Liu, K.-Y.; Hsieh, C.-C.; Yu, J.-S. K.; Liaw, W.-F. *Inorg. Chem.* **2012**, *51*, 10092−10094.
(19) Hsieh, C.-H.; Brothers, S. M.; Reibenspies, J. H.; Hall, M. B.; Popescu, C. V.; Darensbourg, M. Y. *Inorg. Chem.* **2013**, *52*, 2119−2124.
(20) Roncaroli, F.; van Eldik, R.; Olabe, J. A. *Inorg. Chem.* **2005**, *44*, 2781−2790.
(21) (a) Becke, A. D. *Phys. Rev. A* **1988**, *38*, 3098−3100. (b) Perdew, J. P. *Phys. Rev. B* **1986**, *33*, 8822−8824.
(22) (a) Tao, J. M.; Perdew, J. P.; Staroverov, V. N.; Scuseria, G. E. *Phys. Rev. Lett.* **2003**, *91*, 146401−146404. (b) Staroverov, V. N.; Scuseria, G. E.; Tao, J. M.; Perdew, J. P. *J. Chem. Phys.* **2003**, *119*, 12129−12137.
(23) (a) Nakatsuji, H. *Chem. Phys. Lett.* **1978**, *59*, 362−364. (b) Nakatsuji, H. *Acta Chim. Hung.* **1992**, *129*, 719−776. (c) Nakatsuji, H.; Hirao, K. *J. Chem. Phys.* **1978**, *68*, 2053−2065.
(24) (a) Werner, H.-J.; Knowles, P. J. *J. Chem. Phys.* **1985**, *82*, 5053−5063. (b) Knowles, P. J.; Werner, H.-J. *Chem. Phys. Lett.* **1985**, *115*, 259−267.
(25) (a) Angeli, C.; Cimiraglia, R.; Evangelisti, S.; Leininger, T.; Malrieu, J. P. *J. Chem. Phys.* **2001**, *114*, 10252−10264. (b) Angeli, C.; Cimiraglia, R.; Malrieu, J. P. *J. Chem. Phys.* **2002**, *117*, 9138−9153. (c) Angeli, C.; Pastore, M.; Cimiraglia, R. *Theor. Chem. Acc.* **2007**, *117*, 743−754.
(26) Delcey, M. G.; Freitag, L.; Pedersen, T. B.; Aquilante, F.; Lindh, R.; González, L. *J. Chem. Phys.* **2014**, *140*, 174103.
(27) Radoń, M.; Broclawik, E.; Pierloot, K. *J. Phys. Chem. B* **2010**, *114*, 1518−1528.
(28) Boguslawski, K.; Marti, K. H.; Legeza, Ö.; Reiher, M. *J. Chem. Theory Comput.* **2012**, *8*, 1970−1982.
(29) Boguslawski, K.; Jacob, C. R.; Reiher, M. *J. Chem. Theory Comput.* **2011**, *7*, 2740−2752.

■ NOTE ADDED AFTER ASAP PUBLICATION

This paper was published on the Web on October 3, 2014. Figure 3 was replaced, and the corrected version was reposted on October 6, 2014.